Inorg. Chem. **2004**, *43*, 5884–5890

Formation of Complex Three- and One-Dimensional Interpenetrating Networks within Carbodiimide Chemistry: NCN^{2-}-Coordinated Rare-Earth-Metal Tetrahedra and Condensed Alkali-Metal Iodide Octahedra in Two Novel Lithium Europium Carbodiimide Iodides, $LiEu_2(NCN)I_3$ and $LiEu_4(NCN)_3I_3$

Wuping Liao,[†] Chunhua Hu,[†] Reinhard K. Kremer,[‡] and Richard Dronskowski*,[†]

Institut für Anorganische Chemie der RWTH Aachen, Professor-Pirlet-Strasse 1, D-52056 Aachen, and Max-Planck-Institut für Festkörperforschung, Heisenbergstrasse 1, D-70569 Stuttgart, Germany

Received May 1, 2004

Orange-red transparent single crystals of $LiEu_2(NCN)I_3$ and $LiEu_4(NCN)_3I_3$ were synthesized from fluxes of europium iodide, sodium cyanide, sodium azide, and lithium iodide at elevated temperatures and structurally characterized by X-ray diffraction. While $LiEu_2(NCN)I_3$ crystallizes in the cubic system ($Fd\bar{3}m$, $a = 15.1427(17)$ Å, $V = 3472.2(7)$ Å^3, $Z = 16$, R1 = 0.0322), $LiEu_4(NCN)_3I_3$ adopts the hexagonal system ($P6_3/mmc$, $a = 10.6575(11)$ Å, $c = 6.8232(10)$ Å, $V = 671.16(14)$ Å^3, $Z = 2$, R1 = 0.0246). Both extended structures are composed of complex frameworks built from europium tetrahedra coordinated by carbodiimide (symmetrical NCN^{2-}) units on the one side and condensed iodine octahedra around lithium cations on the other. Within $LiEu_2(NCN)I_3$, vertex-sharing of the LiI_6 subunits together with isolated europium tetrahedra results in two three-dimensional networks interpenetrating each other. Within $LiEu_4(NCN)_3I_3$, face-sharing of the europium tetrahedra results in bitetrahedral units which further connect via two opposing vertexes into one-dimensional linkages. Likewise, the LiI_6 octahedra share common faces to also yield one-dimensional linkages that fill the channels between the europium/carbodiimide substructure. The magnetic behavior of both compounds has been determined; the two phases follow Curie–Weiss laws with weak predominantly ferromagnetic exchange between the europium ions and atomic moments characterizing them as essentially divalent.

Introduction

As a fundamental class of compounds being of special importance for synthetic solid-state and also molecular chemistry, cyanamides and carbodiimides have gained increasing attention within the past decade. In fact, a number of alkali-metal, alkaline-earth-metal, transition-metal, and also main-group-metal cyanamides/carbodiimides and dicyanamides were obtained following different synthetic routes. Probably the first crystal structure refinement with satisfying precision was obtained for calcium cyanamide, CaNCN,[1] prepared from the reaction between calcium carbonate and HCN gas; on the industrial scale, however, calcium cyanamide was manufactured from calcium carbide and molecular nitrogen. The other alkaline-earth-metal cyanamides (i.e., MgNCN, SrNCN, and BaNCN), also being carbodiimides from a structural point of view, were prepared by the reaction of melamine with the metal nitrides.[2] Pulham et al. succeeded in synthesizing lithium carbodiimide from a solid-state reaction of Li_2C_2 with Li_3N at 600 °C, finally crystallizing it from liquid lithium.[3] The syntheses of Na_2NCN[4] and K_2NCN[5] were carried out by the reaction of alkali-metal amides with alkali-metal hydrogen cyanamides in a vacuum and

* Author to whom correspondence should be addressed. E-mail: drons@HAL9000.ac.rwth-aachen.de.
[†] Institut für Anorganische Chemie der RWTH Aachen.
[‡] Max-Planck-Institut für Festkörperforschung.

(1) Vannerberg, N. G. *Acta Chem. Scand.* **1962**, *16*, 2263−2266.
(2) Berger, U.; Schnick, W. *J. Alloys Compd.* **1994**, *206*, 179−184.
(3) Down, M. G.; Haley, M. J.; Hubberstey, P.; Pulham, R. J.; Thunder, A. E. *J. Chem. Soc., Dalton Trans.* **1978**, 1407−1411.
(4) Becker, M.; Nuss, J.; Jansen, M. *Z. Anorg. Allg. Chem.* **2000**, *626*, 2505−2508.
(5) Becker, M.; Jansen, M. *Solid State Sci.* **2000**, *2*, 711−715.

10.1021/ic049432r CCC: $27.50
Published on Web 08/12/2004

liquid ammonia, respectively. Similarly, RbHNCN[6] was obtained by the reaction of cyanamide with rubidium amide in liquid ammonia. In an attempt to synthesize indium cyanides containing monovalent indium from InBr and NaCN, an unforeseen route was discovered that led to two new indium carbodiimides.[7] Nonetheless, most metal cyanamides/carbodiimides such as those of Zn,[8] Cd,[9] Hg,[10] Ag,[11] Pb,[12] and Tl[13] were precipitated from aqueous solution of either Na_2NCN or H_2NCN. In addition, a few transition-metal[14] and lead[15] dicyanamides were prepared from aqueous solutions, while alkali-metal (K, Rb)[16] and alkaline-earth-metal[17] dicyanamides were made by ion exchange from Na-$[N(CN)_2]$. There are also some reports on synthetic routes targeted at metal cyanamides using organosilicon carbodiimides as precursor compounds.[18]

It may come as a surprise to the reader that there are only a very few literature examples touching upon rare-earth-metal cyanamide/carbodiimide chemistry. For example, Ln_2O_2NCN (Ln = La, Ce, Pr, Nd, Sm, Eu, and Gd),[19] with layer structures consisting of $Ln_2O_2^{2+}$ sheets spaced by NCN^{2-} ions, was synthesized by firing rare-earth-metal oxides in the presence of carbon and under flowing ammonia gas. Also, the luminescence properties of Eu^{3+}- and Pr^{3+}-doped La_2O_2-NCN were measured.[20] Recently, Reckeweg and DiSalvo reported the synthesis of EuNCN, isotypic with α-SrNCN, starting from EuN, elemental carbon, and NaN_3 at 1300 K.[21] In addition, two rare-earth-metal chloride carbodiimide nitrides, $Ln_2Cl(NCN)N$ (Ln = La and Ce),[22] were obtained by Meyer et al. through solid-state metathesis reactions between $LnCl_3$ and Li_2NCN at 800 °C. In the structure of $Ln_2Cl(NCN)N$, linear chains of edge-sharing Ln_6 octahedra are interconnected by bridging NCN^{2-} units to form a three-dimensional network that contains residual chlorine anions within linear channels.

When exploring rare-earth-metal cyanamide chemistry by ourselves, we slightly modified the cyanide route (successful for indium carbodiimides) to match the rare earth metals by taking appropriate mixtures of metal halides, cyanides, and azides as precursors. Upon doing so for the case of europium, a whole series of cyanamide/carbodiimide compounds were prepared as a function of temperature. For example, EuNCN prepared from europium iodide, sodium cyanide, and sodium azide is accessible at only 1070 K, while the conventional route needs 1300 K.[21] In the following, we present two novel europium carbodiimide compounds that were obtained from fluxes of lithium iodide. Both crystal structures contain europium tetrahedra interconnected with each other by NCN^{2-} carbodiimide ions.

Experimental Section

Synthesis. Samples of $LiEu_2(NCN)I_3$ (**I**) and $LiEu_4(NCN)_3I_3$ (**II**) were synthesized in high yields from the reactions of EuI_2, NaCN (or KCN), NaN_3, and LiI at elevated temperatures. All physical manipulations were performed in a glovebox (MBraun) under dry argon with oxygen and moisture levels well below 1 ppm. EuI_2 (99.9%, Aldrich) was directly used as a reagent, and NaCN (95%, or KCN, 96%, Merck), NaN_3 (99%, Alfa), and $LiI \cdot 2H_2O$ (LiI purity >80%, Merck) were thoroughly dried at 160 °C for 3 days in vacuo; the purities were checked by X-ray diffraction. It is important to follow this procedure because even traces of moisture or oxygen will lead to the formation of the getter compound Eu_4OI_6 due to the extreme oxygen affinity of Eu.[23] The mixtures were transported into tantalum ampules which were sealed with an arc welder and jacketed with quartz glass ampules, both under argon. The samples were heated to 700−880 °C for 3 days and then slowly cooled (about 6 °C/min) to room temperature. Orange-red transparent single crystals of $LiEu_2(NCN)I_3$ and $LiEu_4(NCN)_3I_3$ were obtained from the reactions of EuI_2, NaCN, NaN_3, and LiI in molar ratios of 2:1:1:2 at 880 °C and 2:1:1:1 at 700 °C, respectively; a reliable temperature control is required to yield the intended compositions. $LiEu_4(NCN)_3I_3$ was also obtained using the above educts but with a 2:1:1:2 molar ratio at 800 °C. The crystals could be easily separated from surplus flux crystals due to differences in color and shape.

Crystal Structure Determination. Single crystals were mounted in glass capillaries under argon for X-ray diffraction. All measurements were performed at 293(2) K using a Bruker SMART APEX CCD diffractometer with graphite-monochromatized Mo Kα radiation (λ = 0.71073 Å). The X-ray intensities were corrected with respect to absorption using an empirical procedure.[24] The crystal structures were solved by means of direct methods and refined using anisotropic displacement parameters for Eu and I and isotropic ones for N, C, and Li. The important crystallographic details are compiled in Table 1. Atomic positions and displacement parameters are given in Table 2, and a listing of selected bond lengths is presented in Table 3. More details of the structure determinations may be obtained from the Fachinformationszentrum Karlsruhe, D-76344 Eggenstein-Leopoldshafen, Germany, on quoting the CSD depository numbers 414 000 for **I** and 414 001 for **II**.

(6) Becker, M.; Jansen, M. *Z. Naturforsch.* **1999**, *54b*, 1375−1378.
(7) Dronskowski, R. *Z. Naturforsch.* **1995**, *50b*, 1245−1251.
(8) Becker, M.; Jansen, M. *Acta Crystallogr., C* **2001**, *57*, 347−348.
(9) Baldinozzi, G.; Malinowska, B.; Rakib, M.; Durand, G. *J. Mater. Chem.* **2002**, *12*, 268−272.
(10) (a) Becker, M.; Jansen, M. *Z. Anorg. Allg. Chem.* **2000**, *626*, 1639−1641. (b) Liu, X.; Müller, P.; Kroll, P.; Dronskowski, R. *Inorg. Chem.* **2002**, *41*, 4259−4265.
(11) Becker, M.; Nuss, J.; Jansen, M. *Z. Naturforsch.* **2000**, *55b*, 383−385.
(12) Liu, X.; Decker, A.; Schmitz, D.; Dronskowski, R. *Z. Anorg. Allg. Chem.* **2000**, *626*, 103−105.
(13) Adams, K. M.; Sole, M. J.; Cooper, M. J. *Acta Crystallogr.* **1964**, *17*, 1449−1451.
(14) (a) Manson, J. L.; Kmety, C. R.; Epstein, A. J.; Miller, J. S. *Inorg. Chem.* **1999**, *38*, 2552−2553. (b) Batten, S. R.; Jensen, P.; Moubaraki, B.; Murray, K. S.; Robson, R. *Chem. Commun.* **1998**, 439−440. (c) Manson, J. L.; Lee, D. W.; Rheingold, A. L.; Miller, J. S. *Inorg. Chem.* **1998**, *37*, 5966−5967.
(15) Jürgens, B.; Hoppe, H. A.; Schnick, W. *Solid State Sci.* **2002**, *4*, 821−825.
(16) Irran, E.; Jürgens, B.; Schnick, W. *Chem. Eur. J.* **2001**, *7*, 5372−5381.
(17) Jürgens, B.; Irran, E.; Schnick, W. *J. Solid State Chem.* **2001**, *157*, 241−249.
(18) (a) Riedel, R.; Kroke, E.; Greiner, A.; Gabriel, A. O.; Ruwisch, L.; Nicolich, J. *Chem. Mater.* **1998**, *10*, 2964−2970. (b) Hering, N.; Schreiber, K.; Riedel, R.; Lichtenberger, O.; Woltersdorf, J. *Appl. Organomet. Chem.* **2001**, *15*, 879−886.
(19) Hashimoto, Y.; Takahashi, M.; Kikkawa, S.; Kanamaru, F. *J. Solid State Chem.* **1995**, *114*, 592−594; **1996**, *125*, 37−42.
(20) Holsa, J.; Lamminmaki, R. J.; Lastusaari, M.; Porcher, P.; Sailynoja, E. *J. Alloys Compd.* **1998**, *277*, 402−406.
(21) Reckeweg, O.; DiSalvo, F. J. *Z. Anorg. Allg. Chem.* **2003**, *629*, 177−179.
(22) Srinivasan, R.; Ströbele, M.; Meyer, H. J. *Inorg. Chem.* **2003**, *42*, 3406−3411.
(23) Liao, W.; Dronskowski, R. *Acta Crystallogr., C* **2004**, *60*, i23−i24.
(24) Sheldrick, G. M. *SADABS*; University of Göttingen: Göttingen, Germany, 1996.

Table 1. Crystallographic Data for $LiEu_2((NCN)I_3$ and $LiEu_4(NCN)_3I_3$

	$LiEu_2(NCN)I_3$	$LiEu_4(NCN)_3I_3$
fw	731.59 g/mol	1115.57 g/mol
cryst syst, space group, Z	cubic, $Fd\bar{3}m$, 16	hexagonal, $P6_3/mmc$, 2
unit cell params (Å, Å^3)		
a	15.1427(17)	10.6575(11)
b		
c		6.8232(10)
V	3472.2(7)	671.16(14)
d_{calcd} (g/cm^3)	5.598	5.520
μ (mm^{-1}) (Mo Kα)	24.903	25.313
R1,wR2[a] ($[F_o > 4\sigma(F_o)]$)	0.0322, 0.0778	0.0246, 0.0551

[a] $R1 = \sum||F_o| - |F_c||/\sum|F_o|$; $wR2 = [\sum w(F_o^2 - F_c^2)^2/\sum w(F_o^2)^2]^{1/2}$.

Table 2. Atomic Coordinates and Isotropic Displacement Parameters (Å^2) for $LiEu_2(NCN)I_3$ and $LiEu_4(NCN)_3I_3$

atom	Wyckoff position	x	y	z	U_{eq}[a]
		$LiEu_2(NCN)I_3$			
Eu	32e	0.21799(4)	x	x	0.0154(3)
I	48f	0.42503(9)	1/8	1/8	0.0245(4)
C	16c	0	0	0	0.016(6)[b]
N	32e	0.0462(6)	x	x	0.012(3)[b]
Li	16d	1/2	1/2	1/2	0.041(17)[b]
		$LiEu_4(NCN)_3I_3$			
Eu1	2c	1/3	2/3	1/4	0.0150(3)
Eu2	6h	0.79138(3)	2x	1/4	0.0160(2)
I	6h	0.13314(5)	2x	1/4	0.0192(2)
C	6g	1/2	0	0	0.0145(12)[b]
N	12k	0.5650(4)	2x	0.0266(11)	U_{iso}(C)
Li	2a	0	0	0	0.053(15)[b]

[a] U_{eq} is defined as one-third of the trace of the orthogonalized U_{ij} tensor. [b] U_{iso}.

Table 3. Selected Bond Lengths (Å)[a]

		$LiEu_2(NCN)I_3$			
Eu−N	×3	2.620(8)	Eu−I[d]	×1	3.7142(12)
Eu−I[a]	×1	3.4247 (9)	Eu−I[e]	×1	3.7142(12)
Eu−I[b]	×1	3.4247 (9)	Eu−Eu	×3	3.9829(18)
Eu−I[c]	×1	3.4247 (9)	I−Li	×2	2.9076(6)
Eu−I	×1	3.7142(12)	N−C	×1	1.211(17)
		$LiEu_4(NCN)_3I_3$			
Eu1−N	×6	2.662(7)	Eu2−I[ii]	×1	3.3772(6)
Eu1−I	×3	3.6955(10)	Eu2−I[iii]	×1	3.6851(6)
Eu1−Eu2	×3	4.1157(6)	Eu2−I[iv]	×1	3.6851(6)
Eu2−N	×4	2.612(5)	I−Li	×2	2.9916(8)
Eu2−I[i]	×1	3.3772(6)	N−C[v]	×1	1.214(7)

[a] Symmetry codes: (a) $x - 1/4, 1/4 + y, 1/2 - z$; (b) $1/4 + y, 1/2 - z, x - 1/4$; (c) $1/2 - z, x - 1/4, 1/4 + y$; (d) z, x, y; (e) y, z, x; (i) $1 - y, 2 + x - y, z$; (ii) $1 - x + y, 2 - x, z$; (iii) $1 - x, 2 - y, - z$; (iv) $1 - x, 2 - y, 1 - z$; (v) $x, 1 + y, z$.

Physical Measurements. Infrared spectra were recorded using a Fourier transform Avatar 360 ESP spectrometer (Nicolet). The magnetizations of a sample of approximately 5.4 mg of **I** and of a sample of ca. 6.8 mg of **II** were measured in an MPMS Squid magnetometer (Quantum Design) with magnetic fields **B** of 0.1, 1, and 5 T. The polycrystalline samples were sealed in quartz glass tubes under 1 atm of argon gas to enable sufficient thermal coupling. The precise amount of Eu present in each sample was determined, after the susceptibility measurements had been finished, by ICP analysis (**I**, 2153(5) μg; **II**, 3351(5) μg) such that possible weight errors could not enter the analysis of the magnetic data. The molar magnetic susceptibilities were corrected for the diamagnetism of the closed shells using -216×10^{-6} cm^3/mol for **I** and -292×10^{-6} cm^3/mol for **II** as diamagnetic contributions to the susceptibilities, which were calculated from the appropriate diamagnetic increments of the respective constituents[25] and also from core−electron and bonding increments.[26]

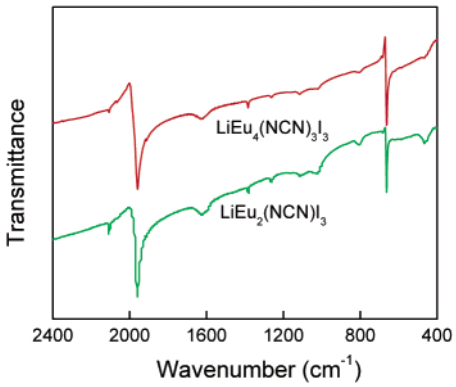

Figure 1. Infrared spectra of $LiEu_2(NCN)I_3$ (bottom) and $LiEu_4(NCN)_3I_3$ (top).

Results and Discussion

Inspired by the reaction of EuN, BN, and NaN_3 to form $Eu_3(NBN)_2$[27] and the synthesis of $In_{2.24}(NCN)_3$[7] from InBr and NaCN, we first chose europium halides, sodium cyanide, and sodium azide as promising precursors for the synthesis of europium cyanamides/carbodiimides. Due to the Eu−X bond strengths (X = Cl, Br, and I) becoming weaker in the order of Cl > Br > I, different products were obtained with different halides using identical thermal conditions. That is to say that equal molar amounts of EuX_2, NaCN, and NaN_3 result in $Eu_2(NCN)Cl_2$ for the chloride case but only Eu(NCN) is formed for the bromide and the iodide. In particular, EuNCN can be synthesized at just 800 °C, while in the literature it is obtained at 1030 °C.

The synthetic temperatures can be further lowered when lithium iodide is utilized as a flux. Then, one arrives at more complex phases, some of which incorporate part of the flux. The formation of $LiEu_2(NCN)I_3$ and $LiEu_4(NCN)_3I_3$ presented here crucially depends on the molar ratios and the applied temperatures:

$$2EuI_2 + NaCN + NaN_3 + LiI \rightarrow LiEu_2(NCN)I_3 + 2NaI + N_2 \text{ (800−880 °C)}$$

$$4EuI_2 + 3NaCN + 3NaN_3 + LiI \rightarrow LiEu_4(NCN)_3I_3 + 6NaI + 3N_2 \text{ (700−800 °C)}$$

The orange-red transparent crystals were first investigated by infrared spectroscopy (Figure 1), and the characteristic vibrational frequencies of the carbodiimide anion (around 1959 cm^{-1} for the asymmetric stretching of NCN^{2-} and 662 cm^{-1} for the deformation vibration of NCN^{2-}) were clearly detected for both compounds and thus immediately confirmed the presence of NCN^{2-}. As required by the selection principle for molecules containing an inversion center, the symmetric stretching is forbidden in the IR spectrum; also,

(25) Selwood, P. W. *Magnetochemistry*, 2nd ed.; Interscience: New York, 1956.
(26) Haberditzl, W. *Angew. Chem., Int. Ed. Engl.* **1966**, *5*, 288−298.
(27) Carrillo-Cabrera, W.; Somer, M.; Peters, K.; von Schnering, H. G. *Z. Kristallogr.—New Cryst. Struct.* **2001**, *216*, 43−44.

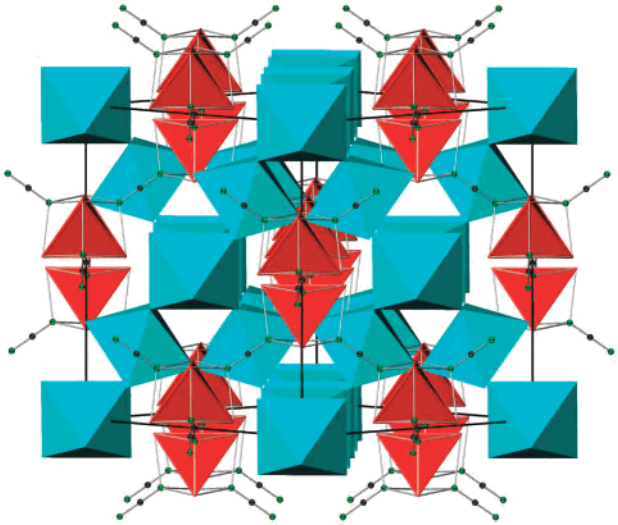

Figure 2. View of the $LiEu_2(NCN)I_3$ structure along [110] showing the two interpenetrating networks of Eu_4/NCN^{2-} and LiI_6 octahedra, with europium tetrahedra given in red, LiI_6 octahedra in blue, nitrogen atoms in green, and carbon atoms in gray.

cyanide contaminations (around 2100 cm^{-1}, strong, and 450 cm^{-1}, medium) are absent. In contrast to the lamellar structure of EuNCN, both materials contain tetrahedral units made up of four europium atoms interspaced by LiI_6 octahedra, but their connectivity patterns differ considerably.

To start with, Figure 2 allows a view into the crystal structure of $LiEu_2(NCN)I_3$ along the [110] direction, and the Eu_4 tetrahedra as well as the LiI_6 octahedra are clearly visible. A straightforward electronic calculation on the basis of an NCN^{2-} unit would yield divalent europium, and there is only one symmetry-inequivalent Eu atom per formula unit (see Table 2). This Eu atom lies on the 32e site and experiences a 9-fold coordination in which there are three nearest nitrogen neighbors (2.62 Å) from NCN^{2-} anions plus six additional iodide anions between 3.42 and 3.71 Å (Table 3). Also, there are three nearest Eu neighbors per Eu atom such that four adjacent Eu atoms form an empty europium tetrahedron which is capped by NCN^{2-} anions on all of its tetrahedral faces (Figure 3, top). The Eu−Eu distance of 3.98 Å almost coincides with the distance in the metal, but this shall not allude to any sizable covalent metal−metal interaction between the Eu^{2+} ions.

As expected from the IR results, the X-ray structure determination yields N−C−N bond lengths and angles (2 × 1.211(17) Å and 180° due to space-group symmetry) that are characteristic for a $D_{\infty h}$-shaped NCN^{2-} unit containing two N=C double bonds; thus, $LiEu_2(NCN)I_3$ can be safely formulated as a carbodiimide. For comparison, we note that the NCN^{2-} unit has been found both in "symmetrical" (carbodiimide) and in "asymmetrical" (cyanamide) configurations, corresponding to the two Lewis formulations $^{-}N{=}C{=}N^{-}$ and $N{\equiv}C{-}N^{2-}$. It is true that the cyanamide molecule, H_2N-CN, exhibits two different molecular bond lengths, namely, 1.15 Å for the C≡N bond and 1.31 Å for the $C-NH_2$ bond,[28] but most metal cyanamides contain a symmetrical, linear carbodiimide unit, for example, in Li_2NCN,[3] $M^{II}NCN$ (M^{II} = Mg, Ca, Sr, Ba),[1,2] and also HgNCN-

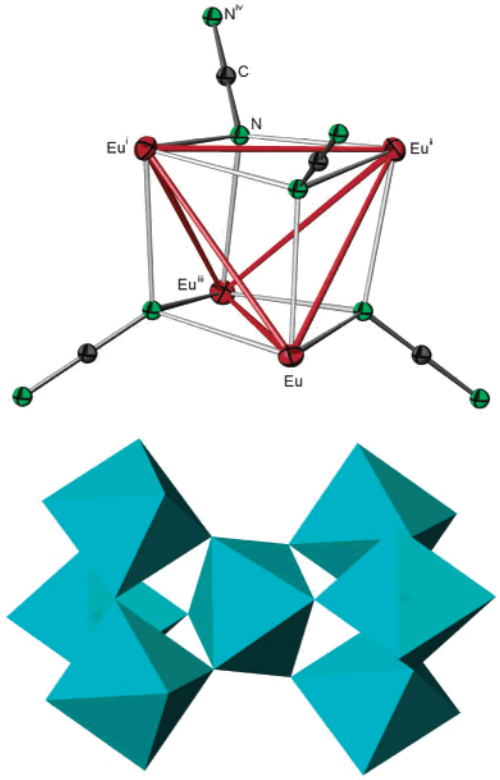

Figure 3. Tetrahedral europium unit in $LiEu_2(NCN)I_3$ capped by NCN^{2-} anions (top) and the interconnection of the LiI_6 octahedra (below). Symmetry codes: (i) $^1/_4 - x, ^1/_4 - y, z$; (ii) $^1/_4 - x, y, ^1/_4 - z$; (iii) $x, ^1/_4 - y, ^1/_4 - z$; (iv) $-x, -y, -z$.

(I).[10] Likewise, EuNCN (with N=C equal to 1.215(12) and 1.229(12) Å, 177.4(9)°) turns out to be a carbodiimide.[21] Only if the chemical bonding between the NCN^{2-} unit and the coordinated metal is sufficiently covalent, is the asymmetrical (cyanamide) configuration preferred, such as in PbNCN,[12] Ag_2NCN,[11] HgNCN(II),[10] and CdNCN,[9] indicative of the somewhat softer nature of the metal.

All isolated europium tetrahedra within $LiEu_2(NCN)I_3$ are interconnected by the NCN^{2-} anions into a three-dimensional network. This is easily visible from a corresponding view with the lithium/iodine substructure momentarily suppressed (Figure 4, top). The *Aufbau* of the latter starts with the lithium atom on the 16d site and six neighboring iodide anions to form an octahedral LiI_6 unit. Each LiI_6 octahedron shares all of its six corners with six adjacent octahedra (Figure 3, bottom) such that all octahedra are part of another three-dimensional network (Figure 4, bottom) which perfectly fills the cavities of the Eu_4/NCN^{2-} unit network. Thus, the structure of $LiEu_2(NCN)I_3$ is the result of two interpenetrating ionic networks, similar to a classic *double salt*. To clearly express the connectivity pattern, the $LiEu_2(NCN)I_3$ formula might alternatively be written as $Eu_4(NCN)_{4/2}{\cdot}(LiI_{6/2})_2$.

The structure of compound **II** exhibits similarities and dissimilarities with the preceding one. As given by Figure 5, one also finds europium tetrahedra and NCN^{2-} units; however, the structural differences between $LiEu_2(NCN)I_3$

(28) (a) Zvonkova, Z. V.; Khvatkina, A. N. *Kristallografiya* **1961**, *6*, 184−189. (b) Denner, L.; Luger, P.; Buschmann, J. *Acta Crystallogr., C* **1988**, *44*, 1979−1981.

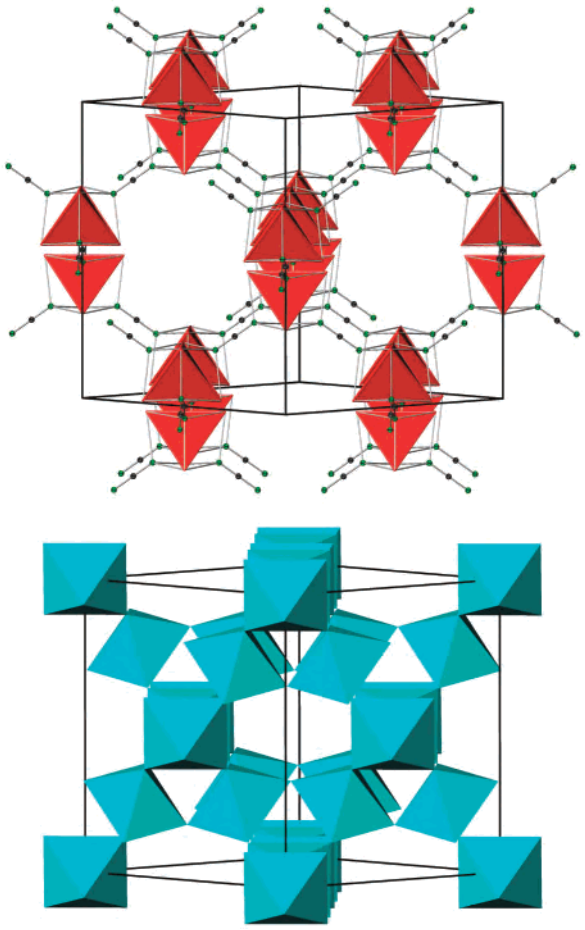

Figure 4. Same as in Figure 2 but decomposing the structure into the two interpenetrating networks.

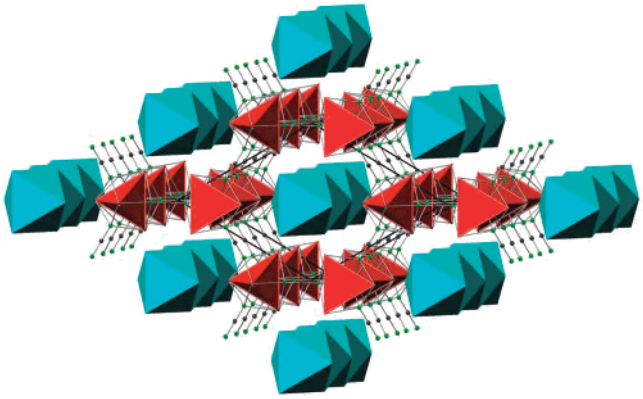

Figure 5. A projection of the crystal structure of $LiEu_4(NCN)_3I_3$ along [001] showing one-dimensional europium channels filled by one-dimensional LiI_6 octahedral chains.

and $LiEu_4(NCN)_3I_3$ become obvious from their surroundings and the connectivity patterns. Within the extended structure, there are two sites for the europium atoms, one at 2c (Eu1) and the other one at 6h (Eu2). The coordination number of Eu1 is nine, six with the nitrogen atoms of the NCN^{2-} anions and three with the iodide anions, while it is eight for Eu2, four with the nitrogen atoms and the other four with the iodide anions. As visualized in Figure 6 (top), a single europium tetrahedron shares one face, formed solely by the Eu2 atoms, such that a bitetrahedral unit is generated. These

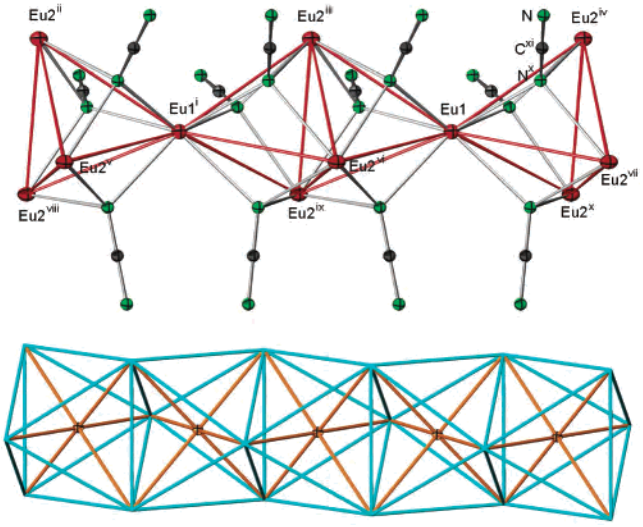

Figure 6. Infinite one-dimensional $[(Eu1)_{2/2}(Eu2)_3]$ chains capped by NCN^{2-} anions (top) and infinite one-dimensional $[LiI_{3/2}I_{3/2}]$ chains formed by LiI_6 octahedra sharing opposite faces (bottom) in $LiEu_4(NCN)_3I_3$. The lithium cations are shown in brown. Symmetry codes: (i) $x, y, z + 1$; (ii) $1 - x, -x + y, 2 - z$; (iii) $1 - x, -x + y, 1 - z$; (iv) $1 - x, -x + y, -z$; (v) $y - 1, -x + y, 2 - z$; (vi) $y - 1, -x + y, 1 - z$; (vii) $y - 1, -x + y, -z$; (viii) $1 - x, 2 - y, 2 - z$; (ix) $1 - x, 2 - y, 1 - z$; (x) $1 - x, 2 - y, -z$; (xi) $x, y + 1, z$.

bitetrahedral units are linked with each other through the cornering Eu1 atom, and each tetrahedral face is also capped by an NCN^{2-} anion. The latter also exhibit N═C distances of $2 \times 1.214(7)$ Å (and also 180° due to space-group symmetry) characteristic for the carbodiimide entity.

The bitetrahedral units are connected into one-dimensional linkages which run along [001], and the bridging NCN^{2-} anions generate a framework such that there are one-dimensional channels to accommodate the LiI_6 octahedra. In contrast to the structure of $LiEu_2(NCN)I_3$, the LiI_6 octahedra inside $LiEu_4(NCN)_3I_3$ also form strictly one-dimensional linkages along [001] by sharing two opposite faces (Figure 6, bottom). Thus, the crystal structure of $LiEu_4(NCN)_3I_3$ is composed of two one-dimensional entities, namely, the Eu_4/NCN^{2-} framework and the linkage of LiI_6 octahedra filling the one-dimensional channels such that the chemical formula can be rewritten as $(Eu1)_{2/2}(Eu2)_3(NCN)_{6/2}\cdot(LiI_{3/2}I_{3/2})$. Alternatively, a view along the [001] direction makes it clear that the europium/carbodiimide/iodide framework exhibits one-dimensional hexagonal channels in which the lithium cations reside (Figure 7). Analogous hexagonal halide channels have been observed in the structures of rare-earth-metal oxyhalides,[23,29] and the diameters fall in the range of 4.37−4.86 Å (atom-to-atom distance). We note that these channels remain empty in the latter oxyhalides. In the present compound, however, the lithium-filled channels exhibit a diameter of 7.51 Å. This large channel size should provide sufficient space to also host other cations; corresponding research targeted at replacing lithium is in progress. The large size also alludes to Li^+ mobility, and a corresponding refinement of the site-occupation factor of Li arrives at 0.7(2),

(29) Schleid, T.; Meyer, G. *Z. Anorg. Allg. Chem.* **1987**, *553*, 231−238; *554*, 118−122. *J. Less-Common Met.* **1987**, *127*, 161−166.

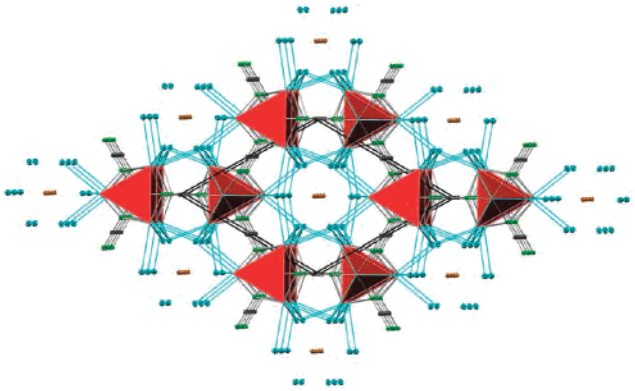

Figure 7. A projection of $LiEu_4(NCN)_3I_3$ along [001] without LiI_6 octahedra showing one-dimensional hexagonal iodide channels and centered lithium cations.

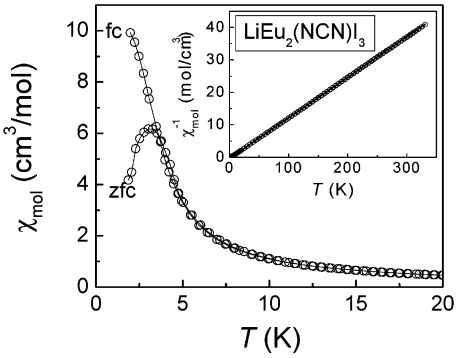

Figure 8. Field-cooled (fc) and zero-field-cooled (zfc) magnetic susceptibility (per Eu atom) of $LiEu_2(NCN)I_3$ determined at 0.1 T. The inset shows the reciprocal molar susceptibility (measured at 1 T) with a fit (solid line) of the Curie−Weiss law $\chi_{mol} = C/(T - \Theta)$ with parameters $C = 8.00(14)$ (cm^3 K)/mol and $\Theta = 2.8(3)$ K.

the high standard deviation reflecting the minute scattering contribution (0.6%). Because the resolution limit has obviously been reached, other methods (transport measurements, solid-state NMR) will be needed to answer the question of ionic mobility.

In agreement with the differing dimensionalities of $LiEu_2(NCN)I_3$ (three-dimensional) and of $LiEu_4(NCN)_3I_3$ (one-dimensional), the connectivities of the iodide anions also differ. Within $LiEu_2(NCN)I_3$, the iodide anion exhibits the I^{i-a-a} functionality[30] by simultaneously bridging one tetrahedral Eu−Eu edge and being coordinated to two vertexes of two other tetrahedra. In $LiEu_4(NCN)_3I_3$, the iodide anion is located over the Eu1 atoms of a bitetrahedron $[(Eu2)_3(Eu1)(Eu2)_3]$, connecting with the Eu1 atom and two Eu2 atoms at both sides. At the same time, it coordinates two Eu2 atoms (I^a) from two other chains.

With respect to the magnetic behavior of the two phases, Figure 8 displays the molar susceptibility (per mole of Eu ions) for **I** below 20 K determined in a field of 0.1 T; Figure 9 shows the corresponding data for **II**. The insets display the reciprocal magnetic susceptibilities determined in a field of 1 T. Measurements in fields up to 5 T showed no magnetic

(30) Schäfer, H.; von Schnering, H. G. *Angew. Chem.* **1964**, *76*, 833−849. Examples for the notation: The ligand X^a is connected only to one vertex of a metal array, X^i bridges one M−M edge, X^{i-a} bridges one edge and is coordinated to the vertex of another cluster, and X^{a-a-a} links three different clusters via their vertexes.

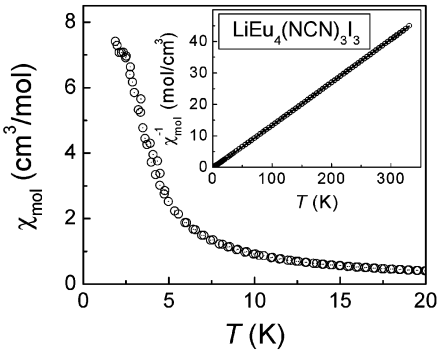

Figure 9. Magnetic susceptibility (per Eu atom) of $LiEu_4(NCN)_3I_3$ determined at 0.1 T. The inset shows the reciprocal molar susceptibility (measured at 1 T) with a fit (solid line) of the Curie−Weiss law $\chi_{mol} = C/(T - \Theta)$ with parameters $C = 6.63(9)$ (cm^3 K)/mol and $\Theta = 1.9(1)$ K.

field dependence of the magnetic susceptibiliy, e.g., due to saturation of possible tiny traces of ferromagnetic impurities.

Above 10 K, the susceptibilities follow Curie−Weiss laws with an effective magnetic moment (per Eu atom) of 8.00(7) μ_B for **I** and 7.65(5) μ_B for **II**. The paramagnetic Curie temperatures amount to 2.8(3) K (**I**) and 1.9(5) K (**II**), both indicating weak predominant ferromagnetic exchange interaction. Below 10 K there are deviations from the Curie−Weiss law which are ascribed to the onset of long-range magnetic ordering effects. For **I** there is a clear splitting of the fc and the zfc magnetization below 3.5(1) K, indicating an irreversibility possibly due to the reorientation of ferromagnetically or weakly ferromagnetically ordered domains. For **II**, fc and zfc data remain identical down to 1.8 K. Both, however, show a slight anomaly at 2.4(2) K, most likely from the onset of long-range antiferromagnetic (afm) ordering.

The effective moment per Eu atom in **I** is in good agreement with the value of 7.93 μ_B expected for all Eu ions being in oxidation state +2 with a spin-only $4f^7$ electronic configuration ($g = 2$). There is some reduction of the effective moment (~3%) in **II**, which indicates that a small fraction (7%) of the Eu atoms are present with an oxidation state of +3. Eu^{3+} with an electronic configuration of $4f^6$ exhibits essentially temperature-independent paramagnetism,[31] which, in the amount under question, is difficult to detect because of the strong temperature-dependent paramagnetism of the majority of the Eu^{2+} ions. It is thinkable, though, that the Eu1 position of $LiEu_4(NCN)_3I_3$ (25% of all europiums involved) is responsible, at least in part, for the lowered moment. A close inspection of Table 3 (see also Figure 6) reveals that the enlarged number of coordinating nitrogen atoms (six N neighbors) can be expected to lead to an also enlarged bond-valence sum for Eu1 in comparison to Eu2 (only four N neighbors). If Eu1 were to get close to the trivalent state, the excess electron would probably be delocalized over the one-dimensional chain of europium tetrahedra, thereby posing no problem for the charge balance of the compound.

In summary, two lithium europium carbodiimide iodides were prepared using a new synthetic route to synthesize

(31) Lueken, H. *Magnetochemie*, B. G. Teubner: Stuttgart−Leipzig, 1999.

cyanamides/carbodiimides with a lithium iodide flux. As the significant structural features both compounds contain three- and one-dimensional frameworks made up of Eu_4 tetrahedra, coordinated by NCN^{2-} anions, and also connected LiI_6 octahedra. Magnetic measurements indicate divalent Eu and long-range ordering below ca. 3 K for both phases.

Acknowledgment. It is a pleasure to thank the Fonds der Chemischen Industrie for their continuous support.

Supporting Information Available: X-ray crystallographic data in CIF format for the structure determinations of $LiEu_2(NCN)I_3$ and $LiEu_4(NCN)_3I_3$. This material is available free of charge via the Internet at http://pubs.acs.org.

IC049432R